Bull. Mater. Sci. (2018) 41:48
https://doi.org/10.1007/s12034-018-1555-9

Structures and electronic properties of W_mCu_n ($n + m \leq 7$) clusters

YU ZHICHENG[1], ZHANG XIURONG[1,*], HUO PEIYING[1] and GAO KUN[2]

[1]School of Mathematics and Physics, Jiangsu University of Science and Technology, Zhenjiang 212003, China
[2]School of Material Science and Engineering, Jiangsu University of Science and Technology, Zhenjiang 212003, China
*Author for correspondence (zh4403701@126.com)

MS received 2 May 2017; accepted 12 June 2017; published online 29 March 2018

Abstract. Geometric and electronic structures of W_mCu_n ($m + n \leq 7$) cluster have been systematically calculated by density functional theory at the generalized gradient approximation level for ground-state structures. W_mCu_n clusters with $n = 1, 3, 5$ tend to form bipyramid structures, whereas WCu_n favour planar shapes except for WCu_5. The configurations of W_mCu_n clusters are more sensitive to the Cu atoms than the W atoms, while the average atomic binding energies and the total magnetic moments are determined by W atoms. The calculated second-order differences in energies and HOMO–LOMO energy gaps show pronounced odd–even oscillating behaviours. From the Mulliken electron population analysis, we found that Cu 4p and W 6p orbitals exhibit electronic charges and both Cu 4s and W 6s orbitals transfer electronic charges to the W 5d orbital, which lead to the extension of W–Cu bond lengths.

Keywords. W_mCu_n ($m + n \leq 7$) clusters; structure and stability; electronic property; density functional theory.

1. Introduction

Atom clusters, acting as an intermediate state between single atom and bulk materials, have been studied physically and chemically on their unique properties for the characters like large specific surface and catalytic activity which are applicable to the use of hydrogen storage, photoabsorption material and catalysts in the electron transfer reduction, etc. [1–6]. For common transition-metal clusters, incomplete d shells dominate their properties [7]. Nevertheless, the d electrons form full d^{10} shells in elements of IB and IIB groups whose properties relate to the delocalized behaviour of the external sp electrons [8,9]. The domination of configurations and electronic properties in alloy-clusters consisting of elements with both incomplete d shell and full d^{10} shell arouse our interest.

In particular, tungsten and copper clusters which belong to the categories mentioned above have been studied extensively both experimentally and theoretically [10–23]. Jug *et al* [19] have studied the structure and stability of small copper clusters, revealing that similar trends are found for the binding energies of Cu_n and Cu^+_{n+1} clusters, which can be explained by the isoelectronic nature of the valence s orbitals. Carrión *et al* [21] have investigated the geometrical, electronic and magnetic properties of W_n ($n = 1-16, 19, 23$) atomic clusters, concluding that tungsten aggregates with $n = 15$ and above exhibit a clear tendency to adopt structures derived from the body-centered cubic system, and mainly singlet, triplet and quintet electronic states characterize small tungsten aggregates.

Different from pure clusters, bimetallic clusters show fickle structures and properties depending on the type of the doped element and the size of clusters [22–28]. Lin *et al* [29] have investigated the structures and energies of copper-doped small silicon clusters $CuSi_n$ ($n = 4-10$) and their anions, showing that adding an additional electron to $CuSi_{10}$ pulls out the Cu atom from the centre location, and forms an exohedral ground-state structure of $CuSi^-_{10}$. Tungsten–copper composite materials doped with graphene were successfully fabricated with the mechanical alloy and pressureless infiltration sintering technology by Dong [30], revealing that graphene reacts with W and forms W_2C and WC during the sintering process when the graphene content is 1.0 wt%. CuW70 alloy was achieved by Gao [31], indicating that a part of W particles are fragmented and become smaller on the surface, while the Cu particles only exhibit deformation.

WCu alloy clusters and materials were vastly experimented, and several studies revealed that small-sized clusters doped with tungsten or copper atoms show the magnetic properties [32–34]. In addition, tungsten clusters are three-dimensional configurations beginning with four atoms, while copper clusters are planar constructions up to six atoms. Thus, clusters having seven and less atoms are the smallest systems including 1D, 2D and 3D growing patterns. To the best of our knowledge, this is the first computational study on this nanoalloy formed by tungsten and copper atoms. In the present work, we report an accurate simulated data and discuss the structures and electronic properties of neutral W_mCu_n ($m+n \leq 7$) clusters.

2. Computational method

The structure optimization of W_mCu_n ($m + n \leq 7$) clusters has been performed using density functional theory

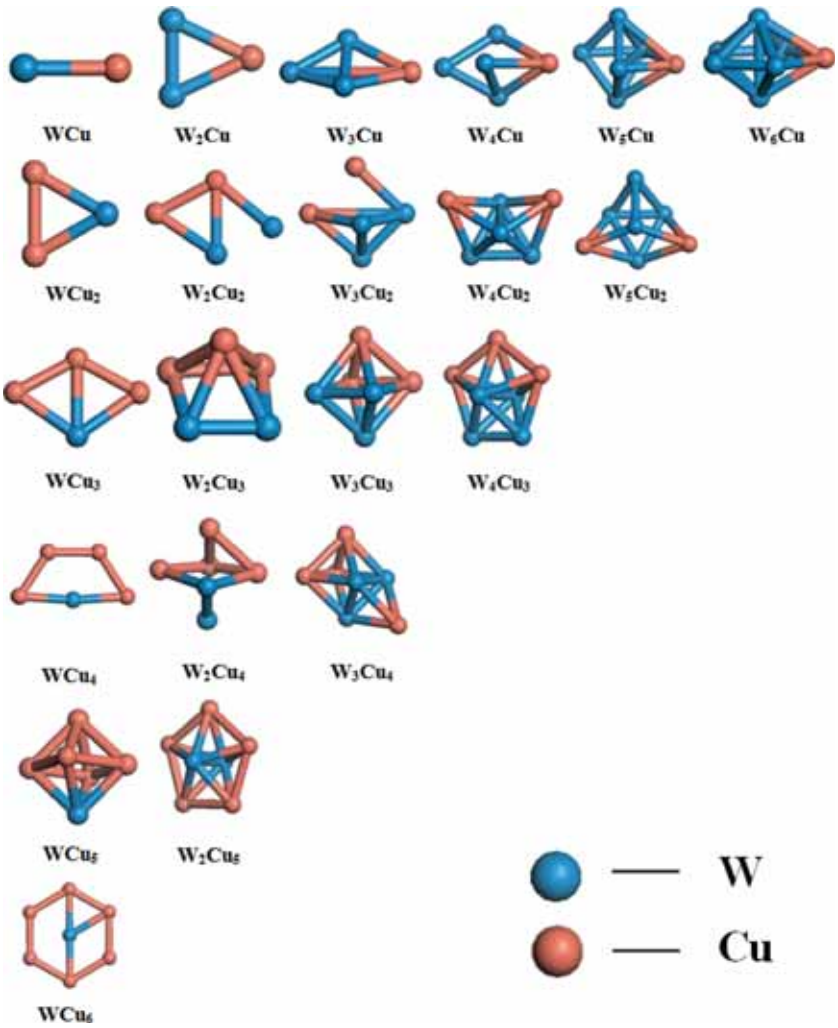

Figure 1. Lowest energy structures of W_mCu_n ($m + n \leq 7$) clusters.

(DFT) method at the generalized gradient approximation (GGA) level [35] in Dmol^3 software package [36,37]. The pseudopotentials for W and Cu were generated using the $5s^25p^65d^46s^26p^0$ and $3s^23p^63d^{10}4s^14p^0$ valence configurations, respectively. In the process of geometric optimization, converge thresholds were set to be 2.0×10^{-5} Hartree for the energy, 0.004 Hartree Å^{-1} for the forces and 0.005 Å for the displacement. Ultimate systems were fully optimized at the exchange correlation functional of Perdew and Wang combined with DNP basis set and DFT semi-core pseudopotentials (DSPP) [38] under the GGA program. All of the possible spin multiplicities of each initial configurations were considered to ensure that the obtained structures are lowest in energy. In order to locate the global minimum and avoiding trapping in the local minimum, a wide variety of trial structures were performed. All the most stable bimetallic clusters obtained were characterized as true minima without imaginary frequencies. The convergence criterion of self-consistent field (SCF) was set to be 10^{-5} Hartree to find the relatively stable configurations. The direct inversion in the iterative subspace (DIIS) was used to accelerate the speed of SCF convergence. Smearing has been considered in calculation at first to find the relatively stable configurations, and the smearing of molecular orbital occupation was set to be 0.002 Hartree. As the value decreases to zero, the lowest-energy structures were found. Charge and spin were set at 1.088 eV nm^{-1} and 0.0005 nm, respectively. All other parameters used the default values. We refer to the ground-state structures of W_n ($n = 2-4$) clusters that our research group has obtained and described in Ref. [22]. To test the accuracy of our method, the dimmers for W_2 and Cu_2 were calculated. For W_2 cluster, the calculated bond length of 2.12 Å and dissociation energy of 3.81 eV are all consistent with the experimental and theoretical data of 2.04–2.16 Å and 3.35–5.0 eV [22,23,39–41]. For Cu_2, the calculated bond length of 2.24 Å and binding energy of 2.07 eV are in good agreement with the data of 2.18–2.26 Å and 1.93–2.22 eV (see Ref. [42] and therein).

Table 1. Symmetry, multiplicity and average bond length of W–W, W–Cu and Cu–Cu for W_mCu_n ($m + n \leq 7$) clusters.

Structure	Symmetry	Multiplicity	$L_{(W-W)}$/Å	$L_{(W-Cu)}$/Å	$L_{(Cu-Cu)}$/Å
WCu	$C_{\infty v}$	6	—	2.46	—
WCu_2	C_{2v}	5	—	2.48	2.52
W_2Cu	C_{2v}	2	2.17	2.55	—
WCu_3	C_{2v}	6	—	2.56	2.38
W_2Cu_2	C_s	1	—	2.55	2.39
W_3Cu	C_s	2	2.33	3.14	—
WCu_4	C_{2v}	1	—	2.52	2.42
W_2Cu_3	C_s	2	2.18	2.54	2.46
W_3Cu_2	C_1	1	2.36	2.84	—
W_4Cu	C_s	2	2.48	2.65	—
WCu_5	C_{4v}	4	—	2.49	2.48
W_2Cu_4	C_{2v}	1	2.20	2.59	2.47
W_3Cu_3	C_{3v}	2	2.37	2.60	2.49
W_4Cu_2	C_{2v}	1	2.47	2.65	—
W_5Cu	C_s	2	2.54	2.81	—
WCu_6	D_{6h}	1	—	2.49	2.49
W_2Cu_5	D_{5h}	2	2.27	2.56	2.70
W_3Cu_4	C_{3v}	1	2.38	2.61	2.51
W_4Cu_3	C_{2v}	2	2.49	2.65	2.57
W_5Cu_2	C_s	1	2.47	2.65	—
W_6Cu	C_{2v}	2	2.57	2.71	—

3. Results and discussion

3.1 *Structures*

The search for most stable configurations of W_mCu_n ($m+n \leq 7$) clusters were conducted as follows. Isomers of pure W_n or Cu_n ($n = 2-7$) were chosen to be the original clusters (refer to Refs. [18,20,22,38,41]). The second step in the present calculation was to optimize the geometry with respect to the total energy of all possible $W_{n-1}Cu$ ($n = 2-7$) clusters resulting from the substitution of a W atom by a Cu atom in all the non-equivalent sites of the stable configurations. Next, the same procedure was carried out beginning with pure Cu_n ($n = 2-7$) clusters and replacing Cu atoms one at a time. After a large number of configuration computation and comparison, the averaged atomic binding energies (E_b), second-order difference of energies (Δ_2E) and HOMO–LUMO gap (E_g) of the ground-state structures are shown in figures 2, 3 and 4.

The global minimum structures for the lowest energy W_mCu_n ($m+n \leq 7$) clusters are displayed in figure 1. Semi-stable state structures have to get enough energy to go over the barrier, so the most stable configurations are meaningful for experimental study of W_mCu_n ($m+n \leq 7$) clusters. Multiplicity, symmetry and the average bond length of W–Cu, W–W and Cu–C0u are listed in table 1.

WCu cluster is a linear consisting of two atoms and a W–Cu bond. W_2Cu, WCu_2, W_2Cu_2, WCu_3, WCu_4 and WCu_6 are all two-dimensional structures, which are connected with the fact that Cu_n ($n \leq 6$) clusters favour planar configurations [43]. In addition, the configuration of WCu_4 is similar to Cu_5 cluster experimented by Bauschlicher *et al* [44]. W_mCu_n clusters with $n = 1, 3, 5$ tend to form bipyramid structures, shown in figure 1 as well. Besides the clusters mentioned above, other W_mCu_n clusters tend to form 3D configurations because of the transformation of the coordination number.

Bond length represents bond strength. The more electrons participate in bond formation, the shorter it will be. Compared with bond length of pure W_2 (2.12 Å) and Cu_2 (2.24 Å), that of WCu (2.46 Å) is significantly lager which represents the smaller interatomic force and may relate to the shielding effect resulting from increase of spin-up electrons in 5d orbital. Among the data from table 2, W–Cu, Cu–Cu and W–W bonds all tend to elongate while W–Cu bonds in W_mCu ($m \geq 3$) are notably larger than that in the others because some electrons transfer from 3d orbital to 4s and 4p orbitals in Cu ($1s^22s^22p^63s^23p^64s^13d^{10}$) atoms, and spin-up electrons appear in 4p and 3d orbitals which interact with spin-up electrons in 5d orbital of W atoms. The increase of number for either W or Cu atoms will lead to the extension of W–Cu, Cu–Cu and W–W bond length, which may be due to the rise of coordination number. It is worth noting that Cu tend to form local planar arrangements in bimetallic clusters and the formation becomes relatively stable with the extension of W–Cu bonds.

Multiplicity is associated with the number of unpaired electrons. In table 1, the multiplicities of WCu, WCu_2, WCu_3 and WCu_5 are dramatically larger than the others.

Table 2. Mulliken electron population analysis for the ground state of W_mCu_n ($m + n \leq 7$) clusters.

Structure	Atom	Charge (a.u.)	Spin (hbar)	Natural electronic configuration
WCu	W(1)	− 0.023	4.961	5s(2.000)5p(5.996)6s(1.209)5d(4.735)6p(0.083)
	Cu(2)	− 0.077	0.039	3s(1.999)3p(5.999)4s(1.180)3d(9.812)4p(0.087)
WCu_2	Cu(1)	− 0.064	− 0.122	3s(1.999)3p(5.998)4s(1.056)3d(9.782)4p(0.165)
	Cu(2)	− 0.064	− 0.122	3s(1.999)3p(5.998)4s(1.056)3d(9.782)4p(0.165)
	W(3)	0.029	4.345	5s(1.999)5p(5.994)6s(1.097)5d(4.693)6p(0.117)
W_2Cu	W(1)	− 0.010	2.027	5s(1.999)5p(5.994)6s(1.176)5d(4.658)6p(0.183)
	Cu(2)	− 0.042	0.117	3s(2.000)3p(5.998)4s(1.028)3d(9.779)4p(0.238)
	W(3)	− 0.048	− 1.144	5s(1.999)5p(5.994)6s(1.313)5d(4.586)6p(0.155)
WCu_3	Cu(1)	− 0.080	0.119	3s(1.999)3p(5.998)4s(1.153)3d(9.766)4p(0.164)
	Cu(2)	− 0.042	0.415	3s(1.999)3p(5.998)4s(0.962)3d(9.780)4p(0.303)
	Cu(3)	− 0.080	0.119	3s(1.999)3p(5.998)4s(1.153)3d(9.766)4p(0.164)
	W(4)	0.102	4.347	5s(2.000)5p(5.995)6s(1.136)5d(4.485)6p(0.282)
W_2Cu_2	W(1)	0.153	1.544	5s(1.999)5p(5.994)6s(1.044)5d(4.619)6p(0.190)
	Cu(2)	− 0.210	0.045	3s(1.999)3p(5.998)4s(1.267)3d(9.808)4p(0.138)
	W(3)	− 0.045	− 1.547	5s(1.999)5p(5.993)6s(1.355)5d(4.600)6p(0.097)
	Cu(4)	0.001	0.058	3s(1.999)3p(5.997)4s(0.905)3d(9.757)4p(0.341)
W_3Cu	W(1)	0.099	0.613	5s(2.000)5p(5.999)6s(1.151)5d(4.519)6p(0.232)
	Cu(2)	− 0.242	0.035	3s(1.999)3p(5.998)4s(1.278)3d(9.798)4p(0.169)
	W(3)	0.099	0.613	5s(2.000)5p(5.999)6s(1.151)5d(4.519)6p(0.232)
	W(4)	− 0.056	− 0.260	5s(2.000)5p(5.998)6s(1.381)5d(4.537)6p(0.104)
WCu_4	Cu(1)	− 0.142	− 0.003	3s(1.999)3p(5.998)4s(1.229)3d(9.767)4p(0.150)
	Cu(2)	− 0.032	0.001	3s(1.999)3p(5.997)4s(1.019)3d(9.745)4p(0.272)
	Cu(3)	− 0.032	0.001	3s(1.999)3p(5.997)4s(1.019)3d(9.745)4p(0.272)
	Cu(4)	− 0.142	− 0.003	3s(1.999)3p(5.998)4s(1.229)3d(9.767)4p(0.150)
	W(5)	0.248	0.104	5s(1.999)5p(5.989)6s(1.129)5d(4.398)6p(0.237)
W_2Cu_3	Cu(1)	− 0.010	0.089	3s(1.999)3p(5.997)4s(0.884)3d(9.739)4p(0.390)
	Cu(2)	− 0.103	0.079	3s(1.999)3p(5.997)4s(1.089)3d(9.742)4p(0.274)
	Cu(3)	− 0.106	0.093	3s(1.999)3p(5.997)4s(1.089)3d(9.744)4p(0.276)
	W(4)	0.061	0.313	5s(1.998)5p(5.994)6s(1.277)5d(4.474)6p(0.195)
	W(5)	0.057	0.426	5s(1.998)5p(5.994)6s(1.294)5d(4.469)6p(0.188)
W_3Cu_2	W(1)	− 0.003	0.010	5s(2.000)5p(5.997)6s(1.353)5d(4.487)6p(0.166)
	W(2)	− 0.004	0.011	5s(2.000)5p(5.997)6s(1.362)5d(4.479)6p(0.166)
	W(3)	0.150	− 0.089	5s(2.000)5p(6.001)6s(1.047)5d(4.498)6p(0.304)
	Cu(4)	− 0.128	− 0.016	3s(1.999)3p(5.997)4s(1.090)3d(9.749)4p(0.292)
	Cu(5)	− 0.115	− 0.016	3s(1.999)3p(5.997)4s(1.073)3d(9.746)4p(0.298)
W_4Cu	Cu(1)	− 0.223	0.016	3s(2.000)3p(5.997)4s(1.209)3d(9.753)4p(0.264)
	W(2)	0.086	0.442	5s(2.000)5p(6.000)6s(6.178)5d(4.362)6p(0.374)
	W(3)	0.003	0.163	5s(2.000)5p(5.999)6s(1.305)5d(4.397)6p(0.296)
	W(4)	0.033	0.229	5s(2.000)5p(6.000)6s(1.255)5d(4.383)6p(0.330)
	W(5)	0.000	0.150	5s(2.000)5p(6.000)6s(1.295)5d(4.400)6p(0.305)
WCu_5	Cu(1)	− 0.015	0.039	3s(1.999)3p(5.997)4s(0.967)3d(9.723)4p(0.328)
	W(2)	0.071	2.907	5s(1.999)5p(5.992)6s(1.357)5d(4.318)6p(0.262)
	Cu(3)	− 0.015	0.039	3s(1.999)3p(5.997)4s(0.967)3d(9.723)4p(0.328)
	Cu(4)	− 0.105	− 0.084	3s(2.000)3p(5.998)4s(1.015)3d(9.818)4p(0.275)
	Cu(5)	− 0.018	0.050	3s(1.999)3p(5.997)4s(0.971)3d(9.723)4p(0.328)
	Cu(6)	− 0.018	0.050	3s(1.999)3p(5.997)4s(0.971)3d(9.723)4p(0.328)
W_2Cu_4	Cu(1)	− 0.033	0.079	3s(1.999)3p(5.997)4s(0.951)3d(9.719)4p(0.367)
	Cu(2)	− 0.127	− 0.006	3s(1.999)3p(5.997)4s(1.068)3d(9.743)4p(0.319)
	Cu(3)	− 0.127	− 0.005	3s(1.999)3p(5.997)4s(1.068)3d(9.743)4p(0.319)
	Cu(4)	− 0.033	− 0.044	3s(1.999)3p(5.997)4s(0.950)3d(9.720)4p(0.366)
	W(5)	0.110	0.038	5s(1.999)5p(5.996)6s(1.281)5d(4.374)6p(0.240)
	W(6)	0.110	0.038	5s(1.999)5p(5.996)6s(1.281)5d(4.374)6p(0.240)
W_3Cu_3	Cu(1)	− 0.121	0.115	3s(1.999)3p(5.997)4s(1.042)3d(9.736)4p(0.348)
	Cu(2)	− 0.122	0.111	3s(1.999)3p(5.997)4s(1.043)3d(9.736)4p(0.347)
	Cu(3)	− 0.121	0.115	3s(1.999)3p(5.997)4s(1.042)3d(9.736)4p(0.348)
	W(4)	0.089	0.185	5s(2.000)5p(5.999)6s(1.231)5d(4.449)6p(0.232)

Table 2. (continued)

Structure	Atom	Charge (a.u.)	Spin (hbar)	Natural electronic configuration
	W(5)	0.088	0.237	5s(2.000)5p(5.999)6s(1.230)5d(4.449)6p(0.234)
	W(6)	0.088	0.237	5s(2.000)5p(5.999)6s(1.230)5d(4.449)6p(0.234)
W_4Cu_2	W(1)	0.080	− 0.031	5s(2.000)5p(6.002)6s(1.210)5d(4.377)6p(0.331)
	Cu(2)	− 0.209	0.001	3s(2.000)3p(5.997)4s(1.199)3d(9.751)4p(0.262)
	W(3)	0.078	− 0.020	5s(2.000)5p(6.001)6s(1.246)5d(4.369)6p(0.308)
	W(4)	0.078	− 0.020	5s(2.000)5p(6.001)6s(1.243)5d(4.369)6p(0.308)
	Cu(5)	− 0.209	0.001	3s(2.000)3p(5.997)4s(1.199)3d(9.751)4p(0.262)
	W(6)	0.080	− 0.031	5s(2.000)5p(6.002)6s(1.210)5d(4.377)6p(0.331)
W_5Cu	W(1)	− 0.020	0.750	5s(2.000)5p(6.005)6s(1.213)5d(4.452)6p(0.350)
	W(2)	0.034	− 0.220	5s(2.000)5p(6.002)6s(1.301)5d(4.476)6p(0.186)
	W(3)	− 0.031	0.639	5s(1.999)5p(6.006)6s(1.212)5d(4.497)6p(0.316)
	W(4)	0.034	− 0.220	5s(2.000)5p(6.002)6s(1.301)5d(4.476)6p(0.186)
	Cu(5)	− 0.161	0.001	3s(1.999)3p(5.997)4s(1.145)3d(9.711)4p(0.309)
	W(6)	0.044	0.049	5s(2.000)5p(6.005)6s(1.222)5d(4.495)6p(0.234)
WCu_6	Cu(1)	− 0.091	− 0.017	3s(1.999)3p(5.997)4s(1.094)3d(9.751)4p(0.250)
	Cu(2)	− 0.091	− 0.017	3s(1.999)3p(5.997)4s(1.094)3d(9.751)4p(0.250)
	Cu(3)	− 0.091	− 0.017	3s(1.999)3p(5.997)4s(1.094)3d(9.751)4p(0.250)
	Cu(4)	− 0.091	− 0.017	3s(1.999)3p(5.997)4s(1.094)3d(9.751)4p(0.250)
	Cu(5)	− 0.091	− 0.017	3s(1.999)3p(5.997)4s(1.094)3d(9.751)4p(0.250)
	W(6)	0.446	2.321	5s(1.999)5p(5.984)6s(0.957)5d(4.345)6p(0.270)
	Cu(7)	− 0.091	− 0.017	3s(1.999)3p(5.997)4s(1.094)3d(9.751)4p(0.250)
W_2Cu_5	Cu(1)	− 0.118	0.071	3s(1.999)3p(5.997)4s(1.090)3d(9.731)4p(0.300)
	Cu(2)	− 0.118	0.071	3s(1.999)3p(5.997)4s(1.090)3d(9.731)4p(0.300)
	Cu(3)	− 0.118	0.070	3s(1.999)3p(5.997)4s(1.091)3d(9.731)4p(0.299)
	Cu(4)	− 0.117	0.069	3s(1.999)3p(5.997)4s(1.092)3d(9.731)4p(0.298)
	Cu(5)	− 0.118	0.070	3s(1.999)3p(5.997)4s(1.091)3d(9.731)4p(0.299)
	W(6)	0.245	0.324	5s(1.999)5p(6.002)6s(1.022)5d(4.400)6p(0.332)
	W(7)	0.245	0.324	5s(1.999)5p(6.002)6s(1.022)5d(4.400)6p(0.332)
W_3Cu_4	W(1)	0.146	− 0.068	5s(2.000)5p(6.001)6s(1.177)5d(4.416)6p(0.261)
	Cu(2)	− 0.128	− 0.002	3s(1.999)3p(5.997)4s(1.051)3d(9.751)4p(0.330)
	Cu(3)	− 0.132	− 0.001	3s(1.999)3p(5.997)4s(1.055)3d(9.750)4p(0.330)
	Cu(4)	− 0.149	0.000	3s(2.000)3p(5.998)4s(1.076)3d(9.785)4p(0.291)
	Cu(5)	− 0.132	− 0.001	3s(1.999)3p(5.997)4s(1.055)3d(9.750)4p(0.330)
	W(6)	0.146	− 0.069	5s(2.000)5p(6.001)6s(1.177)5d(4.416)6p(0.261)
	W(7)	0.149	0.041	5s(2.000)5p(6.001)6s(1.177)5d(4.414)6p(0.259)
W_4Cu_3	Cu(1)	− 0.150	0.032	3s(2.000)3p(5.997)4s(1.091)3d(9.752)4p(0.311)
	Cu(2)	− 0.175	0.069	3s(1.999)3p(5.997)4s(1.123)3d(9.763)4p(0.292)
	Cu(3)	− 0.150	0.032	3s(2.000)3p(5.997)4s(1.091)3d(9.752)4p(0.311)
	W(4)	0.106	0.033	5s(2.000)5p(6.005)6s(1.174)5d(4.407)6p(0.308)
	W(5)	0.082	0.400	5s(2.001)5p(6.002)6s(1.193)5d(4.406)6p(0.317)
	W(6)	0.082	0.400	5s(2.001)5p(6.002)6s(1.193)5d(4.406)6p(0.317)
	W(7)	0.106	0.033	5s(2.000)5p(6.005)6s(1.174)5d(4.407)6p(0.308)
W_5Cu_2	W(1)	0.123	0.031	5s(2.000)5p(6.006)6s(1.115)5d(4.438)6p(0.318)
	W(2)	0.123	0.031	5s(2.000)5p(6.006)6s(1.115)5d(4.438)6p(0.318)
	W(3)	0.031	0.059	5s(2.000)5p(6.005)6s(1.232)5d(4.504)6p(0.228)
	W(4)	− 0.055	0.046	5s(2.000)5p(6.001)6s(1.375)5d(4.558)6p(0.122)
	Cu(5)	− 0.186	0.008	3s(1.999)3p(5.997)4s(1.155)3d(9.760)4p(0.274)
	Cu(6)	− 0.186	0.008	3s(1.999)3p(5.997)4s(1.155)3d(9.760)4p(0.274)
	W(7)	0.049	− 0.285	5s(1.999)5p(6.009)6s(1.142)5d(4.421)6p(0.379)
W_6Cu	W(1)	− 0.079	0.029	5s(2.000)5p(6.004)6s(1.209)5d(4.556)6p(0.229)
	W(2)	0.119	0.465	5s(2.000)5p(6.012)6s(1.088)5d(4.420)6p(0.361)
	W(3)	0.010	0.020	5s(2.001)5p(6.009)6s(1.244)5d(4.575)6p(0.161)
	W(4)	0.119	0.465	5s(2.000)5p(6.012)6s(1.088)5d(4.420)6p(0.361)
	Cu(5)	− 0.200	− 0.008	3s(1.999)3p(5.997)4s(1.152)3d(9.761)4p(0.291)
	W(6)	− 0.002	− 0.007	5s(2.001)5p(6.008)6s(1.247)5d(4.584)6p(0.163)
	W(7)	− 0.067	0.037	5s(2.000)5p(6.005)6s(1.287)5d(4.548)6p(0.227)

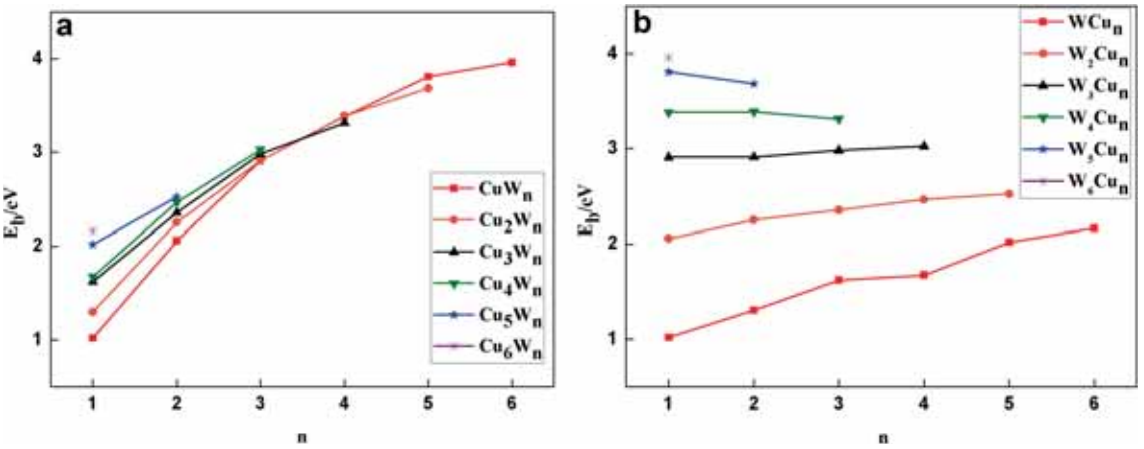

Figure 2. Size dependence of binding energies per atom for the lowest energy structures of W_mCu_n ($m + n \leq 7$) clusters.

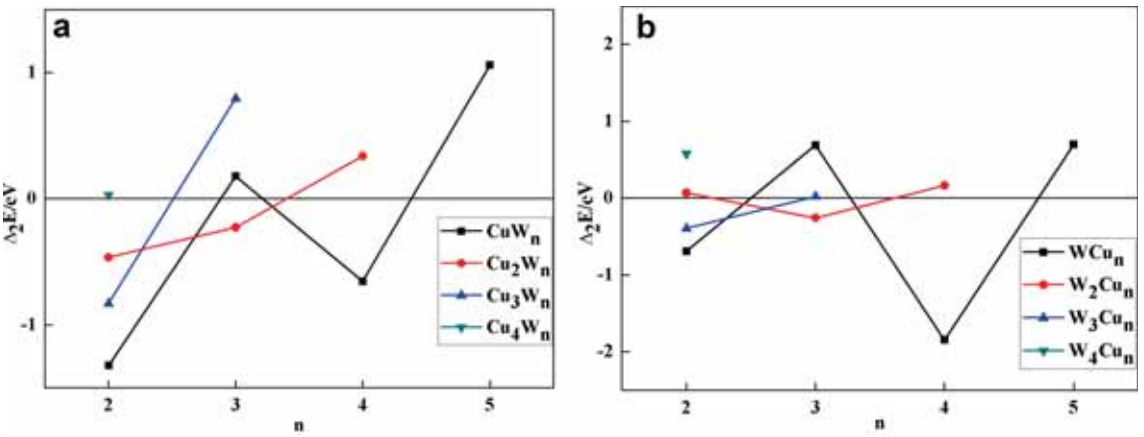

Figure 3. Size dependence of second-order difference of energies for the stable structures of W_mCu_n ($m + n \leq 7$) clusters.

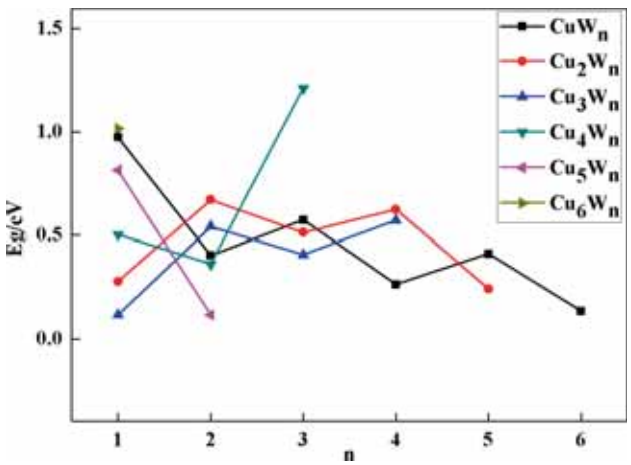

Figure 4. Size dependence of the HOMO–LUMO energy gaps for the stable structures of W_mCu_n ($m + n \leq 7$) clusters.

The related electronic structures have been discussed in section 3.3.

As discussed above, we find that the configurations of W_mCu_n clusters are more sensitive to the Cu atoms than the W atoms. There are few findings about small-sized W_mCu_n clusters to compare with ours. Hence, our results for these clusters should provide a valuable basis for further investigations. Facing the fact that configurations of clusters above are fickle, analysis of stability and electronic properties below can help to account for the evolution of W_mCu_n clusters.

3.2 *Stabilities*

To insight into the relative stabilities, the average binding energies per atom (E_b) and the second-order differences of total energies (Δ_2E) of W_mCu_n ($m + n \leq 7$) clusters based on the lowest-energy configurations have been calculated and

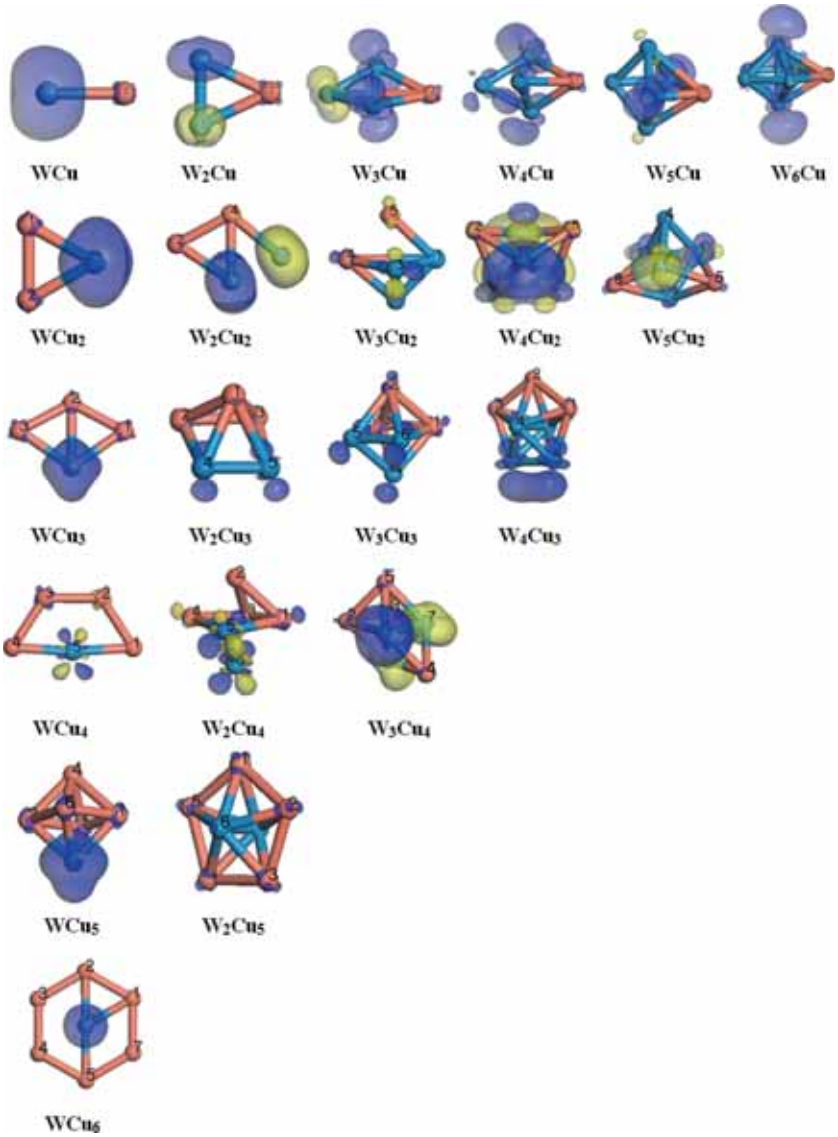

Figure 5. Density of spin electron of W_mCu_n ($m + n \leq 7$) clusters.

presented in figures 2 and 3. E_b and Δ_2E are calculated using the following formulas:

$$E_b(W_mCu_n) = [mE(W) + nE(Cu) - E(W_mCu_n)]/(m+n) \quad (1)$$

$$\Delta_2E = E(W_{m-1}Cu_n) + E(W_{m+1}Cu_n) - 2E(W_mCu_n) \quad (2)$$

$$\Delta_2E = E(W_mCu_{n-1}) + E(W_mCu_{n+1}) - 2E(W_mCu_n) \quad (3)$$

Figure 2a shows the rise of E_b, which depends on the number of Cu atoms in the clusters, and the determinative element in figure 2b is the number of W atoms in the clusters. As is shown in figure 2, when the number of Cu atoms is determined, the average atomic binding energies of W_mCu_n clusters increase monotonically with cluster size. However, when the number of W atoms is determined, the average atomic binding energies of W_4Cu_n and W_5Cu_n clusters decrease with the addition of Cu atoms. The phenomenon may relate to the Coulomb force generated by W atoms. As is known that the proton number of W atom is significantly larger than Cu atom. When the number of W atoms increases up to 4, the repulsive interaction between electrons becomes remarkable leading to the lower binding energy per atom with the increasing number of Cu atoms. Curves in figure 2a overlap with each other but they are smooth with clear gaps in figure 2b, which means that the average atomic binding energies are determined by W atoms. No matter whether the average atomic binding energies of W_mCu_n ($m + n \leq 7$) increase, they display a convergent tendency close to a limit. This means that the larger the cluster is, the smaller the enhanced-stability effect of dopant will be.

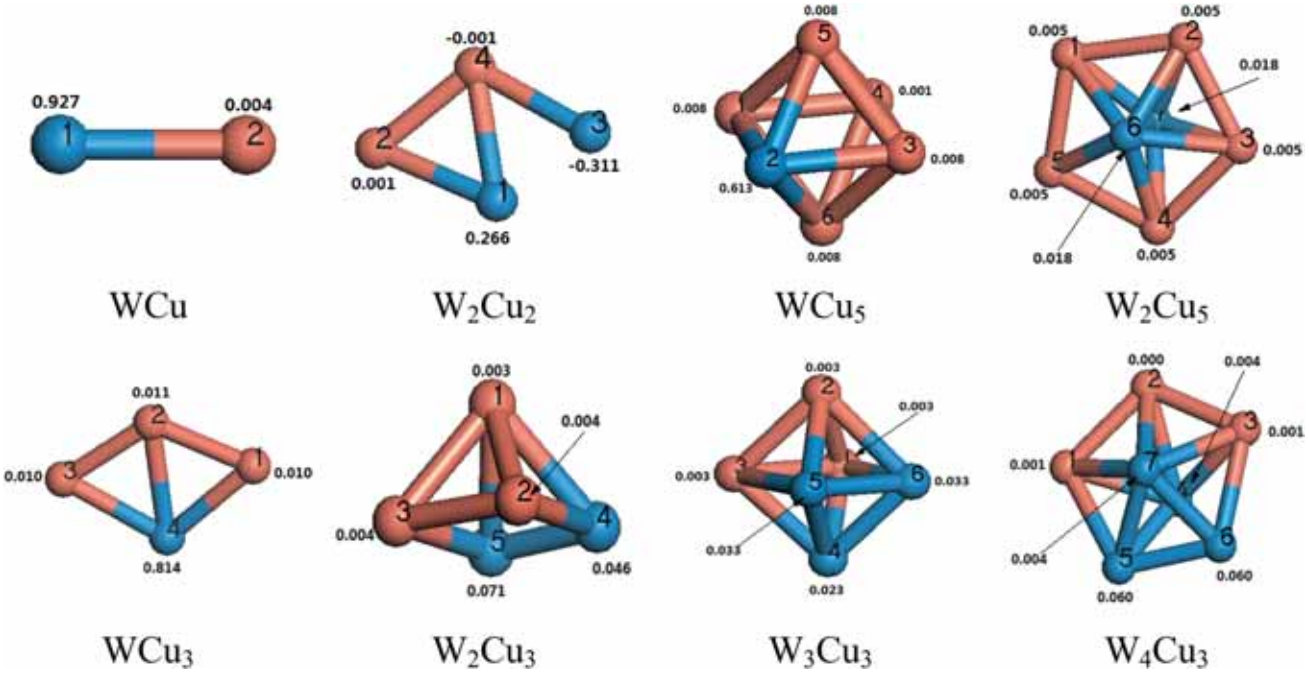

Figure 6. Spin polarization of WCu, W_2Cu_2, WCu_5, W_2Cu_5, WCu_3, W_2Cu_3, W_3Cu_3, W_4Cu_3 clusters at ground state.

The calculated results of Δ_2E as a function of cluster size are plotted in figure 3. Figure 3a shows that the variation tendency depends on the number of Cu atoms in the clusters, and the determinative element in figure 3b is the number of W atoms in the clusters. It is well-known that maximum of Δ_2E is connected with its immediate neighbours and indicates an enhanced stability of a particular cluster. It has been observed that W_3Cu and WCu_3 clusters are more stable than their neighbours, relatively. Furthermore, W_4Cu, WCu_4 and W_2Cu_3 clusters are less stable than their neighbours, respectively. CuW_n, WCu_n and W_2Cu_n clusters all exhibit a pronounced even–odd oscillatory phenomenon with the cluster size increasing. The trends of the curves are in agreement with the results of the average atomic binding energies.

To gain an insight into the electronic stability of W_mCu_n $(m+n \leq 7)$ bimetallic clusters, HOMO–LUMO energy gap, which reflects the ability for electrons to jump from the highest occupied to the lowest unoccupied molecular orbital, as well as the ability for molecule to participate in the chemical reactions to a certain extent has been calculated. And the size dependence of HOMO–LUMO energy gaps for the lowest energy structures of W_mCu_n $(m+n \leq 7)$ clusters are plotted in figure 4.

As can be seen from figure 4, the gap's dependence on the cluster size for W_mCu_n $(m+n \leq 7)$ clusters presents an oscillation between the clusters with even and odd atoms. To be specific, the n-odd $Cu_{1,4,5}W_n$ clusters have higher gaps than n-even ones. The large HOMO–LUMO gap value corresponds to a closed shell electronic configuration and high stability. The gap curves reach relatively large values at WCu, W_3Cu_4, W_3Cu, WCu_4 and W_2Cu_3, indicating that these five clusters own a higher chemical stability than the neighbours. Furthermore, the gaps of W_nCu clusters show a fluctuant downward trend, which is in contrast to the other clusters, revealing that small clusters of W_nCu are more stable than the larger ones.

3.3 *Electronic and magnetic properties*

Table 2 shows the charges and spin of each atom based on the lowest energy structures. The label of atom roots is shown in figure 5. The values of spin equals to the difference of spin up and spin down, which reflect the local magnetic moment of each atom. In the ground state of W_mCu_n $(m+n \leq 7)$ clusters, the spin mainly contributed from W atoms.

By calculating the natural electronic configurations, we found that both 5s and 5p orbitals are nearly filled in W atoms, and 3s together with 3p orbitals are filled in Cu atoms as well among bimetallic clusters W_mCu_n $(m+n \leq 7)$. While W 5d orbital electronic charges increase, the Cu 4p and W 6p orbitals electronic charges appear with increasing number of clusters, which indicate that electronic charges transfer between these orbitals of two types of atoms in bimetallic clusters. From the table, we conclude that Cu 4s and W 6s orbitals contribute some electronic charges to W 5d orbital, W–Cu bonds elongate (compared with data on bond lengths of W–W in Ref. [22]) during the electronic charges transfer at the same time. Due to different valence configurations, copper atoms are considered as a host that provides n delocalized $4s^1$ electrons [45]. Therefore, Cu atoms are usually linked together to cover the W atoms in the ground-state structures of W_mCu_n $(m+n \leq 7)$ clusters calculated in advance. In

addition, all the clusters in the ground multiplet state undergo Jahn–Teller distortion, and tend to distort further towards lower symmetry so as to eliminate their degeneracy and lower their energy. Charges of Cu atoms are often negative except for Cu(4) in W_2Cu_2, and it is a remarkable fact that the charges of two W atoms in this cluster are vastly different. W(1), Cu(2) and Cu(4) can be seen as a group which contributes some electronic charges to W(3), which are the contact between the group and W(3), and Cu(4) still carries positive charges.

Density of spin electron of W_mCu_n ($m + n \leq 7$) clusters, from which the orientation and effects of the electron in the clusters can be seen easily, are shown in figure 5. Blue part represents the density of spin-up electrons and yellow part is the density of spin-down electrons.

It is obvious that the main density of spin electrons root in W atoms which are also the evidence to prove that Cu atom contributes some electronic charges to W atom to enhance the symmetry. Cu_2W_n and Cu_4W_n ($n = 2-7$) show the balance between spin-up and spin-down. Density of spin-up electrons in Cu_3W_n and W_2Cu_5 are distinct from others, which can be discovered from table 2 as well, indicating that each atom in this type of clusters acts as the contributor to the magnetic moment. Of particular note is that WCu, WCu_3 and WCu_5, of which W contributes vast local magnetic moments to the clusters, have larger magnetic moment than the other clusters. Combining table 2 with figure 5, the symmetries of clusters are more visualized.

There is a close relationship between the magnetic moment of clusters and spin multiplicity. The multiplicity (s) and the total magnetic moment (μ) have the following relationship $\mu = s - 1$. The spin of each atom that represents the local magnetic moment is listed in table 2. Compared with pure W clusters, embedding of nonmagnetic Cu atoms promote the spin polarization (SP) of W atoms, so the magnetic moment of the W_mCu_n cluster is increased [26].

To understand further the magnetism of W_mCu_n ($m + n \leq 7$) clusters, the d-electron SP for the clusters were calculated. The SP is determined as shown below [46]:

$$P = (N_{d\uparrow} - N_{d\downarrow})/(N_{d\uparrow} + N_{d\downarrow}), \quad (4)$$

where $N_{d\uparrow(\downarrow)}$represents the number of spin-up (down) d electrons of each atom in the clusters. The SP of each atom in the d orbit of WCu, W_2Cu_2, WCu_5, W_2Cu_5, WCu_3, W_2Cu_3, W_3Cu_3 and W_4Cu_3 clusters mentioned above are shown in figure 6.

As is shown in figure 6, the SP of W atom is distinctly larger than Cu atom that the total magnetic moment mainly comes from W atoms. It is a fact that structures with uniform SP possess good symmetries. The SP of W atoms in W_2Cu_5, W_3Cu_3 and W_4Cu_3 clusters are relatively less than the others, which indicates that the electron transformation between W and Cu atoms in these clusters are relatively little. The SP of W(3) and Cu(4) atoms decrease to negative value, and the SP of W(4) and W(7) are obviously less than W(5) and W(6) in

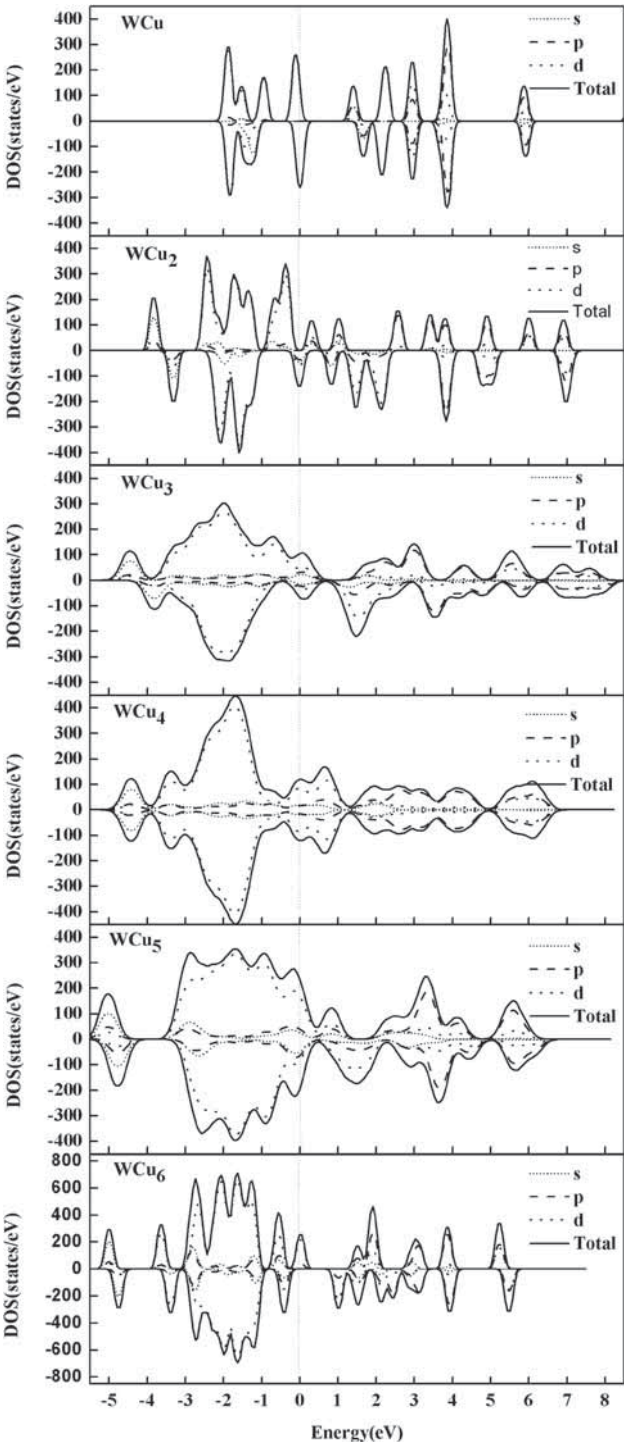

Figure 7. The density of states (DOS) of WCu_n ($n \leq 6$) clusters. The Fermi level is shifted to zero.

W_4Cu_3 cluster, which reveal that the peripheral W atoms are the main source of the total magnetic moment.

In order to investigate the origin of the magnetic step-like behaviour of W_mCu_n clusters, we analyse the projected density of electronic states (PDOS) and the total density of states (TDOS). This study takes the effect of s, p and d orbitals into consideration, because the contribution of f orbital to

the magnetic moment is rarely less. Due to a large magnetic moment jump at WCu, WCu_3 and WCu_5, the WCu_n ($n \leq 6$) were examined and shown in figure 7. As is shown in the diagram, striking hybridization occurs between s, p and d states. It is observed that the total magnetic moments mainly come from s states below the Fermi level because the spin-up and spin-down densities are relatively asymmetry, while the p and d states produce nearly negligible contributions. The hybridization between s, p and d states was observed near the Fermi level for WCu, WCu_3 and WCu_5 clusters. Although the spin-up and spin-down sub-bands of the d states are split, the d states still produce nearly negligible contributions due to the good symmetry of them.

4. Conclusions

The ground-state structures of W_mCu_n ($m + n \leq 7$) clusters were systematically investigated by using DFT method at the GGA level. Stabilities and electronic properties were also calculated based on the most stable structures. The main conclusions are as follows:

(a) W_mCu_n clusters with $n = 1, 3, 5$ tend to form bipyramid structures and Cu atoms tend to encircle the W atoms. The order of the bond lengths is W–Cu > Cu–Cu > W–W as a general rule.
(b) E_b is determined by the proportion of W atoms, and both of Δ_2E and HOMO–LUMO energy gaps exhibit a pronounced even–odd oscillatory phenomenon.
(c) Bond of W–Cu extends during the electronic charges transfer between s, p orbitals of W together with Cu atoms and W 5d orbital.
(d) W contributes vast local magnetic moments to the clusters in WCu, WCu_3 and WCu_5. And the peripheral W atoms are the main source of the total magnetic moments in W_4Cu_3 cluster.

Our calculation focuses upon the small-sized W–Cu clusters which will be a theoretical foundation to experimental study upon TM–W alloy cluster systems. The other medium-sized clusters of this system are also necessary to be experimental researched.

Acknowledgements

This project was supported by the National Natural Science Foundation of China (Grant No. 21207051) and the Graduate Student Research Innovation Program of Jiangsu University of Science and Technology (Grant No. YCX15S-26).

References

[1] İskender M and Ati M 2016 *J. Alloys Compd.* **667** 275
[2] Sun Q and Wang Q 2005 *J. Am. Chem. Soc.* **127** 14582
[3] Wagemans R W P, Lenthe J H V and Jongh P E D 2006 *J. Cheminform.* **127** 16675
[4] Levinger N E, Ray D and Alexander M L 1988 *J. Chem. Phys.* **89** 5654
[5] Wang G C, Jiang L and Morikawa Y 2004 *Surf. Sci.* **570** 205
[6] Zhang X R, Zhang F X and Chen C 2013 *Chin. Phys. B* **22** 123102
[7] Alonso J A 2007 *Chem. Rev.* **100** 637
[8] Alonso J A and March N H 1989 *Academic Press* **7** 563
[9] Alonso J A and Balbás L C 1996 (Berlin, Heidelberg: Springer) 119
[10] Knickelbein M B 1992 *Chem. Phys. Lett.* **192** 129
[11] Powers D E, Hansen S G and Geusic M E 1983 *J. Chem. Phys.* **78** 2866
[12] Lammers V and Borstel G 1994 *Phys. Rev. B* **49** 17360
[13] Fuentealba P 1999 *Chem. Phys. Lett.* **314** 108
[14] Aakeby H, Panas I and Pettersson L G M 1990 *J. Phys. Chem.* **94** 5471
[15] Balbuena P, Derosa P and Seminario J M 1999 *J. Phys. Chem. B* **103** 2830
[16] Calaminici P 1996 *J. Chem. Phys.* **105** 9546
[17] Massobrio C, Pasquarello A and Dal Corso A 1998 *J. Chem. Phys.* **109** 6626
[18] Jackson K A 1993 *Phys. Rev. B* **47** 9715
[19] Jug K, Zimmermann B and Calaminici P 2002 *J. Chem. Phys.* **116** 4497
[20] Jaque P and Toro-Labbe A 2002 *J. Chem. Phys.* **117** 3208
[21] Carrión S M, Pis-Diez R and Aguilera-Granja F 2013 *Eur. Phys. J. D* **67** 1
[22] Zhang X R, Ding X L and Dai B J 2005 *Mol. Struct-Theochem.* **757** 113
[23] Du J, Sun X and Meng D 2009 *J. Chem. Phys.* **131** 044313
[24] Estejab A and Botte G G 2016 *Comput. Theor. Chem.* **1091** 31
[25] Yuan J, Yang B and Li G 2015 *Comput. Mater. Sci.* **102** 213
[26] Zhu J, Zhang H and Zhao L 2016 *Appl. Surf. Sci.* **379** 213
[27] Ping L, Toshiharu T and Kiyotaka A 1999 *J. Phys. Chem. B* **103** 9673
[28] Meitzner G, Via G H and Lytle F W 1987 *J. Chem. Phys.* **87** 6354
[29] Lin L and Yang J 2015 *J. Mol. Model* **21** 5717
[30] Dong L, Chen W and Zheng C 2017 *J. Alloys Compd.* **695** 1637
[31] Gao H, Chen W and Zhang Z 2016 *Mater. Lett.* **176** 181
[32] Hossain D, Pittman C U and Gwaltney S R 2014 *J. Inorg. Organomet. Polymers* **24** 241
[33] Wang J and Han J G 2007 *J. Cheminform.* **38** 12670
[34] Ling W, Dong D and Wang S J 2014 *J. Phys. Chem. Solids* **76** 10
[35] Perdew J P and Wang Y 1992 *Phys. Rev. B* **45** 13244
[36] Delley B 1990 *J. Chem. Phys.* **92** 508
[37] Delley B 2000 *J. Chem. Phys.* **113** 7756
[38] Delley B 2002 *Phys. Rev. B* **66** 155125
[39] Lombardi J R 2002 *Chem. Rev.* **102** 2431
[40] Michael D 1986 *Chem. Rev.* **86** 1049
[41] Wu Z J 2003 *Chem. Phys. Lett.* **370** 510
[42] Poater A, Duran M and Jaque P 2006 *J. Phys. Chem. B* **110** 6526
[43] Li C G, Sun H J and Ren B Z 2016 *Mol. Phys.* **10** 1644
[44] Bauschlicher J, Langhoff S R and Partridge H 1990 *J. Chem. Phys.* **93** 8133
[45] Kuang X J, Wang X Q and Liu G B 2011 *J. Chem. Sci.* **123** 1
[46] Mazin I I 1999 *Phys. Rev. Lett.* **83** 1427